Collision Handling for Humanoids using Proprioceptive Sensing

Jonathan Vorndamme, Moritz Schappler and Sami Haddadin[1]

***Abstract*— High-performance collision handling, is a fundamental robot capability for safe and sensitive operation/interaction in unknown environments, which is divided into the five phases *detection*, *isolation*, *estimation*, *classification* and *reaction*. For complex robots, such as humanoids, collision handling is obviously significantly more complex than for classical static manipulators. In particular, the robot stability during the collision reaction phase has to be carefully designed and relies on high fidelity contact information that is generated during the first three phases. In this work, a unified real-time algorithm capable of determining unknown contact forces and contact locations for humanoid robots is presented. It is based on proprioceptive sensing only, i.e. joint position, velocity and torque, as well as force/torque sensing along the structure. The proposed scheme uses nonlinear model-based momentum observers that are able to recover the unknown contact forces and the respective locations. The dynamic loads acting on internal force/torque sensors are also corrected based on a novel nonlinear compensator. The presented methods are evaluated under various conditions in a simulation of the *Atlas* robot. In summary, we propose a full solution to the problem of *collision detection*, *collision isolation* and *collision estimation* for the general class of humanoid robots.**

I. Introduction and State of the Art

During manipulation tasks, Humanoid robots are usually in contact with their environment at several contact points. E. g. in a bi-manual manipulation scenario, the robot is in contact with its environment at the feet via ground contacts and the hands for executing the desired manipulation. Furthermore, an unwanted contact with a colliding object e.g. at the knee could occur. In order to correctly react to such collisions the robot has to have the ability to detect collisions, analyze the contact situation(s) and react accordingly. In summary, the collision has to be *detected*, *isolated* and *identified*.

Several approaches to the problem of *collision detection* for manipulators exist already. In [16], [14] a model based reference torque is compared to the actuator torque measured via motor currents. An approach with time variant thresholds based on the estimated modeling error can be found in [12], [11], where a generalized momentum based observer is used to estimate the disturbance torques in the joints and also bounds for the modeling errors. Furthermore, many approaches to finding the contact location (*collision isolation*) utilize tactile skins [2], [8], [7], [13]. External joint torque estimation for serial link robots with fixed base was proposed in [5], which was then extended to and validated for flexible joint robots with the DLR lightweight robot in [3]. This was the first method to simultaneously detect collisions, find the contact location and estimate the external torques. The approach utilizes the decoupling property of a generalized momentum based disturbance observer [4], [6], which does not rely on the measurement of accelerations.

In this work, we present the results of [15], where a rigorous model based real-time method for detecting contacts, finding contact locations and estimating the corresponding contact wrenches based on proprioceptive sensing only, is developed. No prior knowledge of the contacts, nor any other simplifying assumptions are required for our scheme. In contrast to previous work, our scheme also incorporates the systematic use of arbitrarily placed load compensated force/torque sensors along the the robot structure. The proposed method is verified in simulation. Overall, the main contributions of this work are

1) the unified solution of the *collision detection, isolation and identification* for humanoid robots based on proprioceptive sensors only,
2) a new real-time method for acceleration estimation and load compensation in humanoid robots for force/torque sensors that are arbitrarily located in the kinematic robot chain,
3) a novel method for estimating contact location and contact forces in single contact scenarios for humanoid robots and the
4) extension to multi-contact situations with and without the help of additional force/torque sensors in the kinematic chain.

This work focuses on the theoretical aspects of the proposed methods. The algorithms are therefore evaluated in basic simulation setups. Current research efforts aim for investigating the robustness of the proposed method in more realistic simulations and real world setups.

TABLE I: Quantities that need to be measured for our detection, isolation and identification algorithm and typical sensors for measuring them.

robot part	measurement quantity	typical sensor
base	$\boldsymbol{\varphi}_B, \dot{\boldsymbol{x}}_B$	gyroscope, Kalman estimator
limbs	$\boldsymbol{\tau}_\mathrm{m}$	joint torque sensor
	$\boldsymbol{\mathcal{F}}_{\mathrm{ext},i}$	force/torque sensor
end-effectors	$\boldsymbol{\mathcal{F}}_{\mathrm{ext},i}$	force/torque sensor

II. Problem Formulation

A. Floating Base Robot Model

A humanoid robot is modeled as

$$\begin{pmatrix}\boldsymbol{M}_\mathrm{BB} & \boldsymbol{M}_\mathrm{BJ}\\ \boldsymbol{M}_\mathrm{JB} & \boldsymbol{M}_\mathrm{JJ}\end{pmatrix}\begin{pmatrix}\ddot{\boldsymbol{q}}_\mathrm{B}\\ \ddot{\boldsymbol{q}}_\mathrm{J}\end{pmatrix}+\begin{pmatrix}\boldsymbol{C}_\mathrm{B}(\dot{\boldsymbol{q}})\\ \boldsymbol{C}_\mathrm{J}(\dot{\boldsymbol{q}})\end{pmatrix}\begin{pmatrix}\dot{\boldsymbol{q}}_\mathrm{B}\\ \dot{\boldsymbol{q}}_\mathrm{J}\end{pmatrix}+\begin{pmatrix}\boldsymbol{g}_\mathrm{B}\\ \boldsymbol{g}_\mathrm{J}\end{pmatrix}= \begin{pmatrix}\boldsymbol{0}\\ \boldsymbol{\tau}_\mathrm{Jm}\end{pmatrix}-\begin{pmatrix}\boldsymbol{0}\\ \boldsymbol{\tau}_\mathrm{Jf}\end{pmatrix}+\begin{pmatrix}\boldsymbol{\tau}_\mathrm{Bext}\\ \boldsymbol{\tau}_\mathrm{Jext}\end{pmatrix} \quad (1)$$

where $\boldsymbol{q}_\mathrm{B} = \begin{pmatrix}\boldsymbol{r}_\mathrm{B} & \boldsymbol{\varphi}_\mathrm{B}\end{pmatrix}^\mathrm{T}$ and $\boldsymbol{q} = \begin{pmatrix}\boldsymbol{q}_\mathrm{B} & \boldsymbol{q}_\mathrm{J}\end{pmatrix}^\mathrm{T}$ denote the base and robot generalized coordinates, consisting of the Cartesian base position $\boldsymbol{r}_\mathrm{B} \in \mathbb{R}^3$, Euler angle base orientation $\boldsymbol{\varphi}_\mathrm{B} \in \mathbb{R}^3$ and joint angles $\boldsymbol{q}_\mathrm{J} \in \mathbb{R}^{n_\mathrm{J}}$. Base and joint entries are marked with index "B" and "J". Further, (1) can be written in the more compact form

$$\boldsymbol{M}(\boldsymbol{q})\ddot{\boldsymbol{q}} + \boldsymbol{C}(\boldsymbol{q},\dot{\boldsymbol{q}})\dot{\boldsymbol{q}} + \boldsymbol{g}(\boldsymbol{q}) = \boldsymbol{\tau}_\mathrm{m} - \boldsymbol{\tau}_\mathrm{f} + \boldsymbol{\tau}_\mathrm{ext}\ , \quad (2)$$

where $\boldsymbol{M}(\boldsymbol{q})$ denotes the mass matrix, $\boldsymbol{C}(\boldsymbol{q},\dot{\boldsymbol{q}})$ the matrix of centrifugal and Coriolis terms, $\boldsymbol{g}(\boldsymbol{q})$ the gravity vector where the dependency on $\boldsymbol{q}$ is left out for brevity in (1). The vectors $\boldsymbol{\tau}_\mathrm{m}$, $\boldsymbol{\tau}_\mathrm{f}$ and $\boldsymbol{\tau}_\mathrm{ext}$ denote the generalized motor, friction and external joint forces. Cartesian forces $\boldsymbol{f}_\mathrm{B}$ and moments $\boldsymbol{m}_\mathrm{B}$ are projected to the base generalized rotation coordinates with the angular velocity Jacobian $\boldsymbol{J}_\omega$ from $\boldsymbol{\omega}_\mathrm{B} = \boldsymbol{J}_\omega(\boldsymbol{\varphi}_\mathrm{B})\dot{\boldsymbol{\varphi}}_\mathrm{B}$.

Generalized external forces $\boldsymbol{\mathcal{F}}_{\mathrm{ext},i}$ are projected via the corresponding geometric floating base Jacobian $\boldsymbol{J}_{C_i}$ of the

[1]The authors are members of the Institute of Automatic Control at Leibniz Universität Hannover, lastname@irt.uni-hannover.de

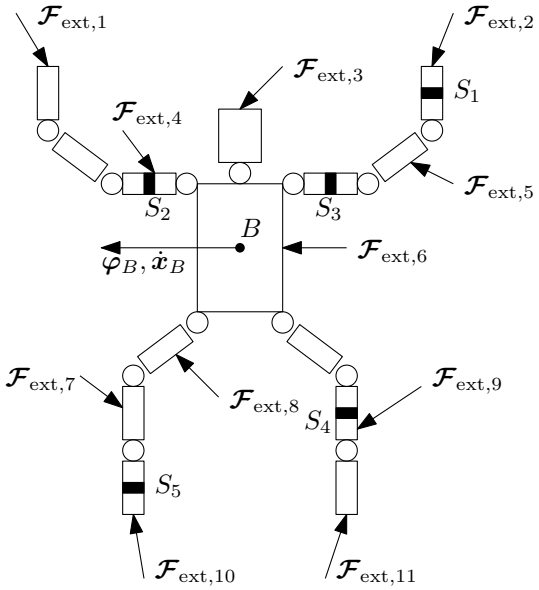

Fig. 1: Considered problem of a humanoid robot in multiple contact situation. Generalized external forces $\mathcal{F}_{\text{ext},i}$ are acting anywhere along its structure. Forces in the feet originate from locomotion, forces at the hands may originate from manipulation. Other external forces are caused by possibly unwanted collisions. Also a number of force/torque sensors S_i (5 in this concrete example) are distributed arbitrarily along the robot structure.

point of contact $\boldsymbol{r}_{C_i}$ to the generalized joint forces

$$\begin{aligned}\boldsymbol{\tau}_{\text{ext},i} &= \begin{pmatrix}\boldsymbol{\tau}_{\text{B},\text{ext},i}\\ \boldsymbol{\tau}_{\text{J},\text{ext},i}\end{pmatrix} = \boldsymbol{J}_{C_i}^{\text{T}}\boldsymbol{\mathcal{F}}_{\text{ext},i} \\ &= \begin{pmatrix}\boldsymbol{I}_3 & -\boldsymbol{S}(\boldsymbol{r}_{BC_i})\boldsymbol{J}_\omega & \boldsymbol{R}\boldsymbol{J}_{\text{Jt}C_i}\\ \boldsymbol{0} & \boldsymbol{J}_\omega & \boldsymbol{R}\boldsymbol{J}_{\text{JR}C_i}\end{pmatrix}^{\text{T}}\begin{pmatrix}\boldsymbol{f}_{\text{ext},i}\\ \boldsymbol{m}_{\text{ext},i}\end{pmatrix},\end{aligned} \tag{3}$$

where $\boldsymbol{J}_{\text{Jt}C_i}$ and $\boldsymbol{J}_{\text{JR}C_i}$ are the corresponding translational and rotational submatrices of the joint Jacobian and $\boldsymbol{R}$ is the rotation matrix from robot base to world frame [10], [1].

B. Collision Detection, Isolation and Identification

Let us assume a humanoid robot model according to section II-A. Furthermore, let the system be equipped with joint torque sensing and an arbitrary number of force/torque sensors anywhere along the kinematic chain, see Fig. 1. In addition, the base orientation $\boldsymbol{\varphi}_B$ and the generalized base velocity $\dot{\boldsymbol{x}}_B$ can be measured. Now the objective is to detect, isolate and identify any collision along the robot structure. In this context, collision *detection* means to generate a number of binary signals telling whether a collision is happening or not at a certain topological part of the robot. *Isolation* denotes to find the contact location $\boldsymbol{r}_{C_i}$ for a collision i. *Identification* aims for estimating the generalized external joint force $\boldsymbol{\tau}_{\text{ext}}$ and the external contact wrenches $\boldsymbol{\mathcal{F}}_{\text{ext},i}$. In summary, the objective is to find all contact locations, the corresponding contact wrenches and telling which parts of the robot are in collision at the given time.

Table I lists the measurement quantities required to solve the problem and provides examples of typical sensors capable of measuring them. Note that the acceleration cannot be measured directly. Therefore, common acceleration sensors are often suffering from drift.

III. Experimental Results

A. General Simulation Setup

We apply our collision detection, isolation and identification scheme to an Atlas robot in simulation consisting of cylinders and cuboids as collision geometry from [9]. We assume perfect measurements of the generalized joint forces and the force/torque sensors unless stated differently. Force/torque sensors are placed at the end-effectors (feet and hands) and before the first arm and leg joints and at the upper torso after the three back joints (see Fig. 2). Furthermore, all acting external forces comply with the assumption of a pushing force and the line of action of the forces is chosen such that it does not intersect any other collision body before the contact point.

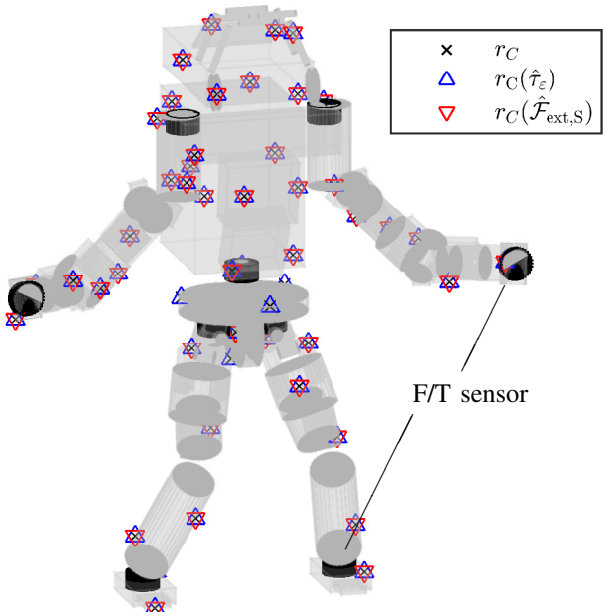

Fig. 2: Distribution of true ($\boldsymbol{r}_{\text{C}}$) and estimated contact locations using two different methods. The points $\hat{\boldsymbol{r}}_{\text{C},\hat{\boldsymbol{\tau}}_\epsilon}$ are isolated using only generalized external joint forces and the points $\hat{\boldsymbol{r}}_{\text{C},\hat{\boldsymbol{\mathcal{F}}}_{\text{ext,S}}}$ are isolated using the force/torque sensor measurements only. For the pelvis (base link) and first torso links, no force measurement is available and therefore contact points at these links cannot be found with the latter method. All overlying points are identical up to rounding errors.

B. Ideal Analysis of Single Contacts

We compare the ideal performance of the isolation based on generalized external joint forces $\hat{\boldsymbol{\tau}}_\epsilon$ to the isolation based only on force/torque sensor measurements $\hat{\boldsymbol{\mathcal{F}}}_{\text{ext},S}$ for a single contact. Dynamic effects due to the observer and load compensation are neglected. The contact points are distributed randomly over the robot surface. Fig. 2 shows the results of the isolation procedures for some representative samples of the 3000 overall tested points. With both methods, the contact points are isolated correctly up to rounding errors, if possible. The contacts at the pelvis cannot be seen by any force/torque sensor and can therefore only be isolated with the generalized external joint forces acting on the base.

C. Ideal Analysis of Multiple Contacts

In the following, we analyze multiple contacts of the type specified in Sec. III-B at the same time.

1) Two Contacts at different links: The points are located at different links, since two contacts at the same link cannot be located in our setup (in order to be able to do so, you would need two force/torque sensors in the same link). 5000 random combinations were examined.

The algorithm using generalized joint forces is able to isolate all two contact point coordinates up to rounding errors if the rank of the stacked contact Jacobian $\boldsymbol{J} = (\boldsymbol{J}_{JC_1} \quad \boldsymbol{J}_{JC_2})^{\text{T}}$ is sufficiently high, i.e. $\text{rank}(\boldsymbol{J}) = 12$ for $N_{\text{C}} = 2$ contact points. Fig. 3 shows the success of the isolation for different contact links, which is equivalent to the plot of the rank deficit

$$RD = 6N_{\text{C}} - \text{rank}(\boldsymbol{J}). \tag{4}$$

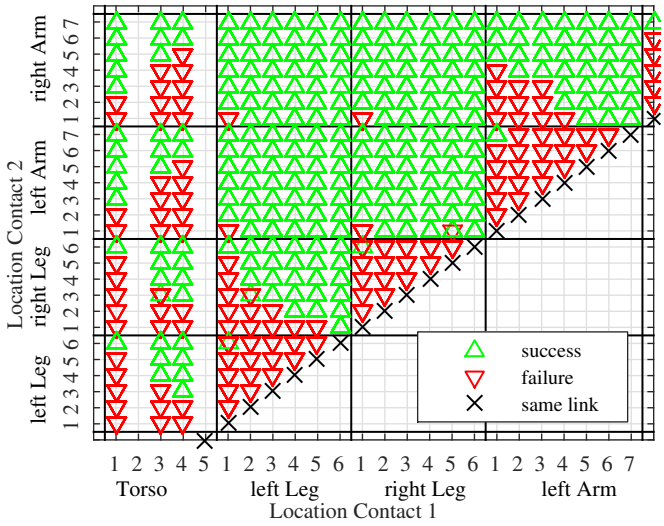

Fig. 3: Overview of success and failure for the isolation of two simultaneous contacts. The x-axis gives the first contact link and the y-axis the second one. The second and the last body of the torso chain have no collision body in the model, the according columns are therefore left empty. A green upward triangle marks the successful isolation of both contact points for the given combination. A red downward triangle marks a combination for which it was impossible to isolate the contacts correctly due to rank loss of the combined Jacobian. In some fields both, green and red triangles are plotted meaning that for this combination the isolation was only partly correct. For the combination of the fifth link in the right leg and the first link of the right arm, this is due to the fact that for some contacts, the joint torque threshold for the last joint is not exceeded and the algorithm is therefore started with a loss of rank in the Jacobian. However, when reducing the joint torque threshold or starting the algorithm with the correct contact links, this could not be observed anymore. In the other cases, the contact point was estimated correctly by chance with a rank deficient Jacobian. Overall 5000 combinations have been tested.

For example, contact one at the pelvis (torso chain link 1) and contact two at the left lower leg (left leg chain link 4) does only produce 10 nonzero columns in the stacked Jacobian and the isolation fails (see corresponding entry in Fig. 3). If instead the foot on the left leg chain (link 6) is in contact, then 12 nonzero columns exist and the isolation succeeds.

For a rank deficit, the isolation method minimizes the Cartesian error of the stacked identified force and finds contact points on the whole following kinematic chain.

2) Contacts at four end-effectors: For our 30 DoF humanoid, it is possible to detect up to $N_\mathrm{C} = 5$ contacts, if the rank deficit RD is zero. This is the case for a typical manipulation scenario with four contacts at the end-effectors of every kinematic chain (feet, hands) and an additional contact located at the torso or first shoulder link.

Without rank deficit, the isolation is successful in all but 5 of the 5000 examined points. The errors occur in situations, where the joint torque threshold for the last joint in at least one chain is not exceeded. This leads to a Jacobian with rank-deficit for the first iteration step of the algorithm, making it in a few cases impossible to find the correct contact link. However, if the threshold is reduced to 10^{-5} N or Nm ($\|\boldsymbol{f}_{\mathrm{ext},i}\| < 1$ N), or the algorithm is started with perfect information about the contact links, no errors occur.

3) Benefits of additional force/torque sensors: The results show the benefits of supplementary force/torque sensors which are summarized in Table II. Without force/torque sensors, up to five contacts can be detected, isolated and identified correctly under certain conditions. With force/torque sensors in the distal links, at least the generalized external manipulation and locomotion forces can be found and further contacts can be isolated by additional force/torque sensors (max. one per sensor) or the first method (up to 5 in theory).

TABLE II: Possibilities of collision detection, isolation and identification with different numbers of force/torque sensors in the kinematic tree. The sensors are meant to be added up down the lines of the table.

sensors	possibilities
only joint torque and base movement sensors	identify ground contact and manipulation contacts, detect single collision, isolate and identify single collision under certain conditions
distal force/torque sensors	full elimination of ground contact and manipulation forces, detection isolation and identification of single collisions, multiple collisions can be detected, isolated and identified in many cases
additional force/torque sensors in the kinematic chains	detect isolate and identify one additional contact wrench per additional sensor

IV. Conclusion

In this work, we propose a unified theoretical framework for collision detection, isolation and identification of generalized external forces acting along a humanoid robot. Apart from standard proprioceptive sensing, the proposed scheme makes use of joint torque measurements and acceleration estimates. Noticeably, it is shown how a generalized momentum observer may be used to calculate these quantities. As the consequential next step, information from load-compensated force/torque sensors, which can be located arbitrarily along the robot structure, is integrated. Considering ideal measurements it is shown that estimating the position of a single contact for humanoid robots is possible without any additional sensors. The positions of multiple concurrent contacts may be estimated with additional force/torque sensors, or, under certain conditions, even without additional sensors.

Future work will cover analyzing the robustness of our scheme in more realistic simulations, in particular with respect to model uncertainties and parasitic sensor effects, as well as real world setups. Furthermore, we will analyze the further systematic fusion of joint torque and force/torque sensing in the collision handling context.

References

[1] K. Bouyarmane and A. Kheddar. On the dynamics modeling of free-floating-base articulated mechanisms and applications to humanoid whole-body dynamics and control. *Humanoids*, 2012.

[2] R. S. Dahiya, P. Mittendorfer, M. Valle, et al. Directions toward effective utilization of tactile skin: A review. *IEEE Sensors Journal*, 2013.

[3] A. De Luca, A. Albu-Schäffer, S. Haddadin, and G. Hirzinger. Collision detection and safe reaction with the DLR-III lightweight manipulator arm. In *IROS*, 2006.

[4] A. De Luca and R. Mattone. Actuator failure detection and isolation using generalized momenta. In *ICRA*, 2003.

[5] A. De Luca and R. Mattone. Sensorless robot collision detection and hybrid force/motion control. In *ICRA*, 2005.

[6] H.-B. Kuntze, C. Frey, K. Giesen, and G. Milighetti. Fault tolerant supervisory control of human interactive robots. In *IFAC Workshop on Advanced Control and Diagnosis*, 2003.

[7] V. J. Lumelsky and E. Cheung. Real-time collision avoidance in teleoperated whole-sensitive robot arm manipulators. *IEEE Transactions on Systems, Man, and Cybernetics*, 1993.

[8] G. D. Maria, C. Natale, and S. Pirozzi. Force/tactile sensor for robotic applications. *Sensors and Actuators A: Physical*, 2012.

[9] Open Source Robotics Foundation. "DRC simulator", https://bitbucket.org/osrf/drcsim. [Online], 2015.

[10] C. Ott, B. Henze, and D. Lee. Kinesthetic teaching of humanoid motion based on whole-body compliance control with interaction-aware balancing. In *IROS*, 2013.

[11] V. Sotoudehnejad and M. R. Kermani. Velocity-based variable thresholds for improving collision detection in manipulators. In *ICRA*, 2014.

[12] V. Sotoudehnejad, A. Takhmar, M. R. Kermani, and I. G. Polushin. Counteracting modeling errors for sensitive observer-based manipulator collision detection. In *IROS*, 2012.

[13] M. Strohmayr. *Artificial Skin in Robotics*. PhD thesis, Karlsruhe Institute of Technology, 2012.

[14] K. Suita, Y. Yamada, N. Tsuchida, et al. A failure-to-safety "kyozon" system with simple contact detection and stop capabilities for safe human-autonomous robot coexistence. In *ICRA*, 1995.

[15] J. Vorndamme, M. Schappler, and S. Haddadin. Collision detection, isolation and identification for humanoids. In *ICRA*, 2017.

[16] Y. Yamada, Y. Hirasawa, S. Huang, et al. Human-robot contact in the safeguarding space. *IEEE/ASME Transactions on Mechatronics*, 1997.